Evidence of coexisting Kondo screening and valence fluctuations in the CePd$_7$/Pd(001) surface alloy

M. Mulazzi,[1,][*] K. Shimada,[2] J. Jiang,[2] H. Iwasawa,[2] and F. Reinert[1,3]

[1]*Universität Würzburg, Experimentelle Physik VII, Am Hubland, D-97074 Würzburg, Germany*
[2]*Hiroshima Synchrotron Radiation Center, Hiroshima University, Higashi-Hiroshima 739-0046, Japan*
[3]*Karlsruhe Institute of Technology KIT, Gemeinschaftslabor für Nanoanalytik, D-76021 Karlsruhe, Germany*

We report on the electronic structure of a clean, well ordered CePd$_7$ surface alloy that was grown in a unique $(\sqrt{5} \times \sqrt{5})R26.6°$ structure, as evidenced by low-energy electron diffraction and Auger electron spectroscopy. Resonant photoemission measurements at the $4d \to 4f$ absorption edge evidenced strong Ce $4f$ derived states having two components near the Fermi level. This observation can be explained by considering very different hybridizations between Ce $4f$ and the Pd $4d$ electrons in the surface and deeper layers. In the former, the hybridization is weak and leads to a spin-dependent screening with low Kondo temperature, while in the latter the hybridization recovers the value of bulk alloy and thus leads to strong charge fluctuations.

I. INTRODUCTION

The physical properties of materials containing rare-earth elements are usually determined by characteristic energy scales, as a consequence of the interactions between the itinerant conduction electrons and the localized f states. Electrons in the f states experience a strong on-site Coulomb repulsion, which is often several times larger than the f bandwidth itself. One of the effects giving a decisive contribution to the macroscopic properties of rare-earth systems is the Kondo effect [1,2], i.e., a spin-dependent scattering increasing the electrical resistivity with decreasing temperature, contrary to the behavior of a normal metal.

The ground state properties and the spectral function of f-electron systems can be described with high accuracy [3–5] by two theoretical approaches, namely the Gunnarson-Schönhammer model [6,7] and the noncrossing approximation (NCA) [8,9] based on the single impurity Anderson model (SIAM). Neither of the methods takes into account the detailed (single particle) band structure of the system, but they use the integrated density of states for the conduction band instead.

So far, most of the electron spectroscopy experiments have been carried out using bulk single crystals, whose surface preparation involves scraping, fracturing in vacuum. These treatments yield the angle-integrated spectra revealing the main features of the Kondo effect, although forbidding the observation of the band dispersion [10]. Cleavage of single crystals can lead to clean and ordered surfaces, but with unknown termination [11–13]. An alternative method consists of growing surface alloys of Ce on a transition metal substrate and using widespread characterization techniques providing clear information about the surface morphology, long-range order, termination, and stoichiometry [14–19]. Following this approach, we prepared the surface alloy of Ce on a Pd(001) substrate, characterized it by low-energy electron diffraction (LEED) and the stoichiometry by Auger electron spectroscopy (AES). The reason why we focused on it is that previous spec-

troscopic studies collocated this alloy in the valence fluctuation regime [20,21], but subsequent work [22,23] showed that there is a non-negligible degree of localization of the $4f$ electrons lying in the surface layer. This experimental finding hints at a possibly different surface electronic structure with respect to the bulk, due to the reduced dimensionality and coordination. Based on this knowledge, we carried out high-resolution resonant angle-resolved photoemission (ARPES) experiments at the N_4 absorption edge of Ce, finding new features in the electronic structure at the Fermi level (E_F) that can be ascribed to a Kondo peak stemming from the surface and a mixed-valence peak originating from the deeper layers of the alloy.

II. EXPERIMENTAL DETAILS

The measurements were carried out at the beamline BL-1 of the HiSOR storage ring at the Hiroshima University. It delivers linearly polarized photons in the 20–400 eV energy range and is equipped with a VG Scienta R4000 analyzer, a cryostat able to reach a minimum temperature of 9 K, and a six-degrees-of-freedom manipulator. The total energy resolution (monochromator plus electron energy analyzer) was measured to be 26 meV when using a photon energy of 122 eV. All the measurements were taken with the p polarization. The Pd(001) sample was cleaned by repeated Ar ion sputtering and 600 °C annealing cycles, as also described in [24]. The substrate was checked by AES, which found no contamination from oxygen, carbon, and sulfur, while LEED showed only the (1×1) pattern with no reconstructions. Metallic Ce was evaporated from an e-beam source at a rate of 8 monolayers (ML) per hour.

Figure 1 shows the AES data measured from the clean Pd crystal and after two subsequent evaporation of a Ce layer, each of a different thickness, as indicated in the figure. The fingerprints of each element are the Pd *MNN* transitions at 323, 270, and 237 eV and the lines of Ce *NOO* at 84 eV and *MNN* at 660 eV, consistent with reference spectra [25] and increasing with the evaporated quantity. However, the AES data of Fig. 1 show O, at a kinetic energy of 530 eV, which was not removable by post-annealing or by evaporating Ce on the hot Pd crystal. To identify the AES signal of Ce, Pd,

─────────
[*]Present address: Humboldt Universität zu Berlin, Institut für Physik, Newtonstr. 15, D-12489, Berlin, Germany; mmulazzi@physik.hu-berlin.de
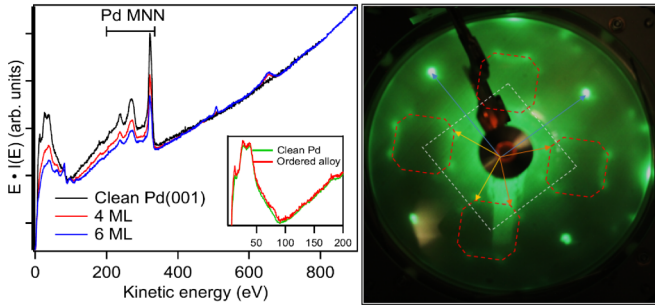
FIG. 1. (Color online) (Left) AES data for the clean Pd substrate and two Ce coverages of 4 and 6 ML on the clean Pd(001) substrate. The peak at 84 eV derives from the Ce *NOO* transition and the one at 660 eV from the Ce *MNN* transition. The strong peaks at 237, 270, and 323 eV are the Pd *MNN* lines, marked in the figure. In the inset it is possible to observe the small contribution of the Ce *NOO* line in the ordered alloy. (Right) LEED pattern of the clean CePd$_7$ alloy obtained after annealing at 600 °C measured with electrons of 56 eV kinetic energy. The pattern can be attributed to a $(\sqrt{5} \times \sqrt{5})R26.6°$ reconstruction with two rotational domains. In the figure, the light blue arrows indicate the reciprocal lattice vectors of the (1×1) surface. The orange and yellow arrows indicate the reciprocal lattice vectors of the $(\sqrt{5} \times \sqrt{5})R26.6°$ reconstruction, whose signature is the octagonal diffraction patters marked by the red dashed lines.

and O from the datasets, a principal component analysis [26] was used. By means of this statistical technique, and assuming that only three component were actually contributing to the spectra, it was possible to determine that the total amount of oxygen evaporated was less than 0.05 ML per monolayer of evaporated Ce.

Given the impossibility of removing the oxygen by the post-evaporation treatment, a more sophisticated preparation was devised to obtain the clean and ordered alloy. Namely, after the evaporation, the sample was post-annealed to favor the interdiffusion of Ce into the Pd, then briefly sputtered to remove the O on the surface and then again annealed at the temperature used for the bare substrate to form the clean and ordered alloy. Thereafter no O was measured by AES, and LEED showed a single $(\sqrt{5} \times \sqrt{5})R26.6°$ reconstruction. In the inset of Fig. 1, the AES data corresponding to the alloy are shown with the clear presence of the Ce *NOO* peak at about 84 eV energy. The weakness of this peak suggests that a very small amount of Ce is present in the sample, thus the formation of a diluted alloy. Evidence of alloying instead of a layer-by-layer growth of Ce on Pd is the behavior of the Pd *MNN* peaks versus the Ce thickness. The growth of the two Ce coverages of Fig. 1, 4 and 6 ML, and a mean escape depth of 8 Å would result in attenuations of 76% and 95% for the Pd peaks. Experimentally, the intensity increase of the Ce peaks is accompanied by a decrease of only 2/3 and 1/2 in the Pd ones (relative to the clean Pd case), much smaller than expected from the layer-by-layer growth mode, excluding the formation of pure Ce layers on the surface of Pd. The actual stoichiometry was obtained in the following way. By the principal component analysis procedure it was possible to obtain the Auger spectrum of the pure Ce and of the pure Pd. The intensity of the pure relative to the alloyed Ce *NOO* peaks yielded the relative Ce density, weighted on the inelastic
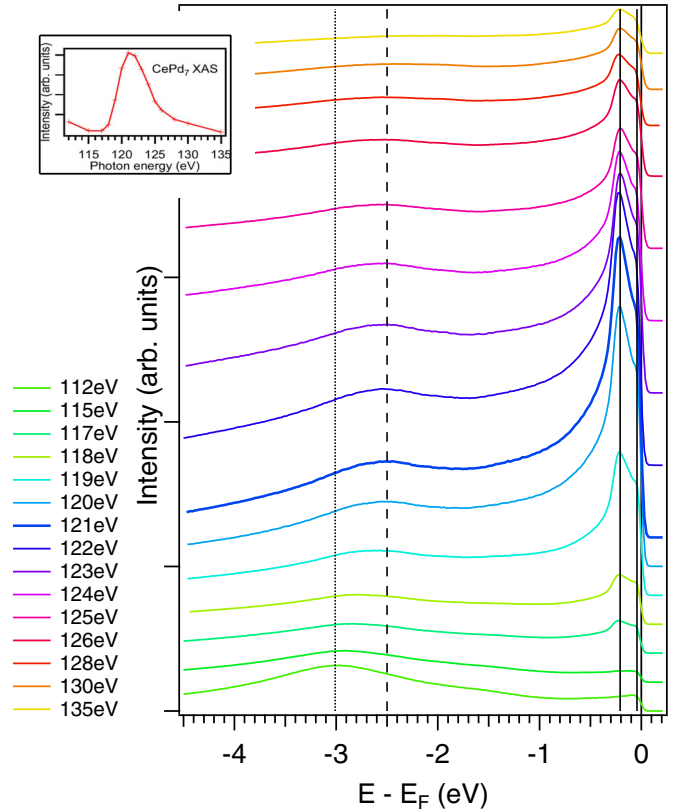
FIG. 2. (Color online) Photoemission data taken for different photon energies across the $4d \rightarrow 4f$ threshold. Each energy distribution curve (EDC) was measured at $T = 9$ K, integrating over the detector acceptance angle. With increasing photon energy, a two-component peak (marked by the continuous vertical lines) near E_F increases strongly and a broad feature at about -2.5 eV (marked by a dashed vertical line) develops, overlapping with the Pd density of states (marked by a dotted vertical line). The inset shows the integral of the photoemission data, proportional to the absorption rate, as a function of the photon energy.

mean free path. The latter was assumed to be 8 Å. From the LEED pattern, which shows only one reconstruction, we assumed that the alloy stoichiometry was constant within the information depth of LEED. This allowed us to conclude that the alloy is in the CePd$_7$ phase. The LEED showed a unique pattern after the second post-annealing that can be attributed to the $(\sqrt{5} \times \sqrt{5})R26.6°$ superstructure, with two coexisting rotational domains.

III. PHOTOEMISSION DATA

Figure 2 show resonant photoemission data obtained varying the photon energy across the $4d \rightarrow 4f$ absorption egde of Ce. As the photon energy increases from 112 to 122 eV, photoemission intensity within 300 meV from the E_F is rapidly increasing in intensity. We observe that this peak, corresponding to a $4f^1$ final state, has actually two components, one at $E \sim 200$ meV and the other one just at the E_F. The broad feature that is observed at higher binding energies throughout the whole photon energy range is attributed to a mixed contribution of the Pd density of states, indicated by a

vertical dotted line in Fig. 2 and of an f^0 satellite (vertical dashed line) that resonates with the photon energy. When the photon energy is increased up to 135 eV, the $4f$ peaks retain a sizable, although reduced, intensity, as also shown in the inset of Fig. 2.

These data are in agreement with previous resonant photoemission experiments [15]: in both experiments the photon energies at which the photoemission intensity has its maximum are the same within 1 eV, the overall photoemission spectra are very similar, and a non-negligible remaining intensity at photon energies higher than the resonance can be observed. However, near the E_F, a new peak is observed, which is important for the discussion of the low-energy excitations in $CePd_7$.

We note that the lineshape of the resonant photoemission (ResPES) data is different from the one observed in other alloys of Ce with Pd. For instance, in the $CePd_3/Pd(111)$ case [27], the ionization peak at a binding energy of about 1 eV is as intense as the $4f^1$ near the E_F. In our case, the $4f^1$ peak is much larger than the $4f^0$, whose energy is larger.

The ARPES data in Fig. 3 present the off- and on-resonance (at 112 and 122 eV) measurements, each of which is sensitive to different parts of the electronic structure. The nonresonant spectrum shows sharp dispersing bands that can be attributed to Pd. In the resonant spectrum we observed an intense flat band
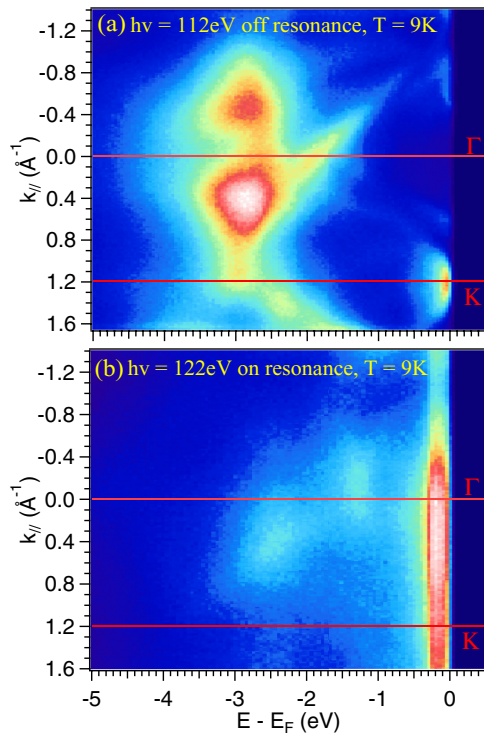
FIG. 3. (Color online) ARPES measurements taken at two energies: (a) off resonance at 112 eV and (b) on resonance at 122 eV. The EDCs presented in Fig. 2 are extracted from datasets similar to those presented in this figure. In (a) mainly the strongly dispersing Pd $4d$ bands are measured, while the Ce $4f$ states are negligible. Conversely, in (b) the f states near the E_F dominate the spectrum, and at higher binding energies an intensity distribution without prominent peaks is measured.
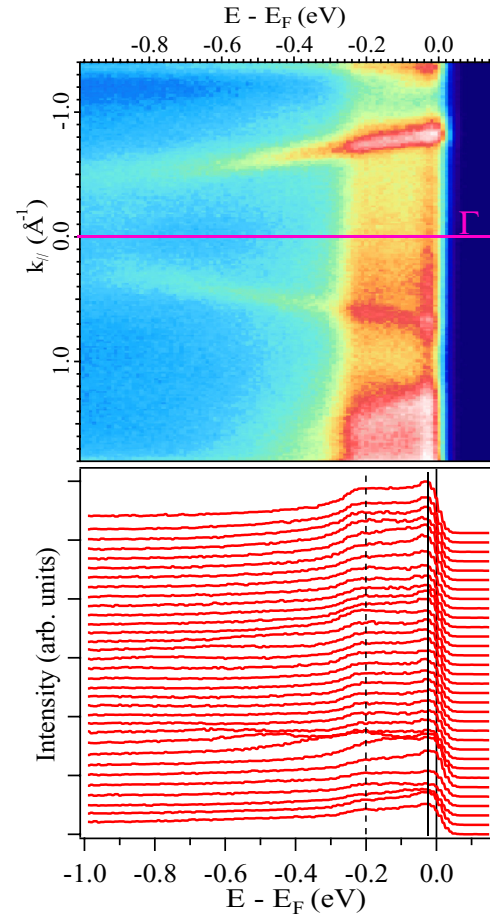
FIG. 4. (Color online) (Top) Resonant ARPES measurements taken at a photon energy of 122 eV with a higher energy resolution showing the details of the electronic structure near the E_F and near the Γ point indicated by the purple line. The strong dispersing bands that cross the E_F at $k_{//} = \pm 0.8$ Å^{-1} are conduction electron states; the nondispersive feature near the E_F is the surface Kondo resonance and the other one at -200 meV is the bulk mixed valence peak. (b) EDCs extracted from (a) starting from $k_{//} = -1.4$ Å^{-1}, with a step of 0.1 Å^{-1} up to $k_{//} = 1.8$ Å^{-1}. The vertical bars indicate the nondispersive peaks near E_F (continuous) and $E_B = 200$ meV (dashed).

near the E_F, originating from the strongest peaks of Fig. 2, and a blurred-out intensity distribution at higher binding energies.

While the ARPES data measuring a wide binding energy range are useful to show the overall band dispersion, Fig. 4 presents the bands near the E_F which are responsible for the low-temperature behavior of this material. As anticipated in Fig. 2, within the first 300 meV from the E_F, two bands are observed: one at about the E_F and the other at 200 meV, neither of them showing a dispersion, and having comparable intensities. The energy positions of these non-dispersive $4f$ states are shown in Fig. 4(b).

IV. DISCUSSION

The interpretation of the experimental data is based on the hybridization between the $4f$ electrons and the conduction electrons of Pd, related to the Kondo temperature, and on

the energy position of the peaks relative to the E_F. The hybridization strength can be determined by x-ray photoemission measuring the Ce $3d$ core levels and analyzing the strength of the f^2 satellite [28,29] relative to the others. For the present experiment, such a measurement was not possible because of the photon energy range limitations of the beamline. Although a measurement of the $4d$ core levels would have been possible, it does not yield a quantitative estimation of the parameters since the spin-orbit energy of this shell is too small to separate the $4d_{3/2}$ from the $4d_{5/2}$ peaks [30]. As found out by model calculations, an alternative way to quantify the hybridization strength is the measurement of the relative strength between the Kondo peak at the E_F and the spin-orbit satellite [31]. Although a comparison of calculations to experiment is rigorous only with momentum-integrated data, this approach proved to be useful also with ARPES measurements [32].

While one may be tempted to attribute the peak in Fig. 4 at 200 meV to a spin-orbit satellite, we deem it unlikely because the binding energy of the spin-orbit peak is an intra-atomic quantity taking a value of about 280 meV in a very wide variety of Ce compounds [10,29,31,33–36]. It would seem a very peculiar case that the binding energy of the spin-orbit satellite of the CePd$_7$ surface alloy examined in this work differed by about 40% from the expected value.

An alternative approach would consist of considering the energy scales of the charge fluctuations in this compound, which were estimated by core-level photoemission [15] showing that their energy is relatively small in CePd$_7$, about 0.5 eV. In the same papers, the authors showed that covering the surface with 1 ML of Pd completely quenches the surface contribution enhancing the hybridization, thus the Kondo temperature, and revealing the mixed-valent nature of the bulk of the alloy. From the theoretical point of view [37–39], the spectral function of a mixed-valent system shows that the f^0 final state exists and can have its maximum in the occupied states, as for the case of the present experiment. For this reason we ascribe the peak at -200 meV to a mixed-valence contribution originating from the deeper layers of the alloy. This attribution implies that the hybridization of the f electron with the conduction band in the bulk is very large, and so is Kondo temperature, which was estimated to be $k_B T_K \approx 1$ eV [15,23] by spectroscopic experiments, in agreement with bulk probing data.

A detail deserving attention is the radical change in the Ce $3d$ core-level spectrum upon deposition of one monolyer of Pd [15]. This evidence can be explained by a change of the electronic structure of the Ce ions due to the presence of new nearest neighbors. In fact, there would be no reason for a strong change in the f^0 peak if the Ce ions were already bonded to Pd, as a next-to-nearest neighbor interaction would have a minimal effect on the Ce core-level spectrum. Based on these considerations we conclude that the first monolayer of the alloy contains Ce atoms. The lower coordination of the Ce atoms at the surface leads to a reduced hybridization and higher occupancy of the $4f$ state, giving rise to the screening of the local moments within the first surface layer. The hypothesis of a different valence in the surface layer with respect to the bulk is corroborated by thermodynamic [21] and spectroscopic experiments [22,23]. The former found evidence of an almost

valence-4 Ce in the bulk, α-like, due to an extremely high hybridization. In spite of this, inverse photoemission spectroscopy data showed the localization of the f electrons at the surface, thus concluding that the surface Ce is γ-like. In the latter experiments, featuring a surface sensitivity that is similar to ours, the authors could also quantify the relative weight of the surface-to-bulk contributions to be at least 40%.

The observation of a Kondo peak at the E_F must be accompanied with the presence of an f^0 satellite. This is actually measured in the resonant photoemission data in Fig. 2 in which a broad peak at a binding energy of 2.4 eV develops with increasing photon energy together with the peak near the E_F. This is clearly distinguished by the density of states of Pd having its maximum at about -3 eV.

The high resolution resonant ARPES (ResARPES) data show clearly the presence of the peak at a binding energy of 200 meV, which was not observed in Ce-based alloy, and a peak at the E_F that was not observed in the previous studies of the CePd$_7$ alloy. These are new findings in this class of deeply studied systems.

Crucial to this observation is the use of a surface-sensitive technique, which allowed us to discover that the depth-dependence of the hybridization in this system is so strong as to give rise to the Kondo effect in the first monolayer of the alloy, whose signature is the peak at the E_F, and to valence fluctuations in the deeper layers, which are signaled by the 200 meV peak. The peak has been reported only on CePd$_7$ so far, to the best of our knowledge [15]. Since we attribute it to bulk valence fluctuations, it would be useful to carry out ResARPES experiments at high resolution on other strongly hybridized surface alloys.

There are three reasons why the Kondo peak has been observed in our experiments, in spite of the fact that previous experiments were carried out in conditions comparable to the present ones. The first reason is that we could prepare a very well ordered alloy on which it was possibleto observe a clear LEED pattern; the second reason is that the energy and angular resolutions in our experiments (25 meV and 0.2°) are higher than those of the past investigations; the third is the lower experimental temperature, 9 K.

The effect of the surface order should not be confused with the formation of a coherent state in the system due to interaction between the $4f$ sites. In the temperature range explored, CePd$_7$ is not in the coherent state, but is in the Kondo regime. The surface order is, however, very important for the determination of the actual intensity and energy of the Kondo peak. This has been shown in several studies that compared the spectra of cleaved and scraped samples, the latter showing a reduction of the Kondo peak intensity with respect to the former.

Given our experimental resolution 25 meV and the temperature, we estimate that the Kondo temperature has to be on the order of 5 K, allowing the effects of the spin scattering to be measurable at 9 K, but to be completely washed out at temperatures higher than 15 K. We stress that the accuracy of this estimate is hindered by the energy resolution of our experiments, which is larger than $k_B T$. A quantitative determination of the Kondo temperature will be done in the future, by systematic measurements of the detailed temperature-dependent data. Another possibility would be to

fit the resonant lineshape with theoretical NCA calculations, an approach that proved to be very successful when probing the momentum-integrated data [3]. However, the calculation of the k-resolved spectral function to analyze angle-resolved photoemission spectra is not feasible at the moment.

V. CONCLUSION

We have presented detailed experimental results about the structure, the electronic band dispersion, and the importance of many-body effects in the surface alloy $CePd_7$. By means of Auger spectroscopy and low-energy electron diffraction we have determined the stoichiometry of the alloy and the lattice superstructure, respectively. Photon energy dependent ARPES data across the $4d$ edge showed that the $4f$ density of states near the E_F shows two overlapping peaks: one is derived from the mixed-valent bulk of the alloy and the other is assigned to the first surface layer, where the different environment of the Ce atoms results in the characteristic small energy scales of the Kondo regime.

[1] J. Kondo, Progr. Theor. Phys. **32**, 37 (1964).

[2] A. Hewson, *The Kondo Problem to Heavy Fermions* (Cambridge University Press, Cambridge, 1993).

[3] F. Reinert, D. Ehm, S. Schmidt, G. Nicolay, S. Hüfner, J. Kroha, O. Trovarelli, and C. Geibel, Phys. Rev. Lett. **87**, 106401 (2001).

[4] D. Ehm, S. Hüfner, F. Reinert, J. Kroha, P. Wölfle, O. Stockert, C. Geibel, and H. von Löhneysen, Phys. Rev. B **76**, 045117 (2007).

[5] M. Klein, J. Kroha, H. v. Löhneysen, O. Stockert, and F. Reinert, Phys. Rev. B **79**, 075111 (2009).

[6] O. Gunnarsson and K. Schönhammer, Phys. Rev. Lett. **50**, 604 (1983).

[7] O. Gunnarsson and K. Schönhammer, Phys. Rev. B **28**, 4315 (1983).

[8] N. E. Bickers, D. L. Cox, and J. W. Wilkins, Phys. Rev. B **36**, 2036 (1987).

[9] T. A. Costi, J. Kroha, and P. Wölfle, Phys. Rev. B **53**, 1850 (1996).

[10] A. Sekiyama, T. Iwasaki, K. Matsuda, Y. Saitoh, Y. Onuki, and S. Suga, Nature (London) **403**, 396 (2000).

[11] J. D. Denlinger, G.-H. Gweon, J. W. Allen, C. G. Olson, M. B. Maple, J. L. Sarrao, P. E. Armstrong, Z. Fisk, and H. Yamagami, J. Electron Spectrosc. Relat. Phenom. **117-118**, 347 (2001).

[12] D. V. Vyalikh, S. Danzenbächer, Yu. Kucherenko, C. Krellner, C. Geibel, C. Laubschat, M. Shi, L. Patthey, R. Follath, and S. L. Molodtsov, Phys. Rev. Lett. **103**, 137601 (2009).

[13] D. Ehm, F. Reinert, G. Nicolay, S. Schmidt, S. Hüfner, R. Claessen, V. Eyert, and C. Geibel, Phys. Rev. B **64**, 235104 (2001).

[14] W. Schneider, S. L. Molodtsov, M. Richter, Th. Gantz, P. Engelmann, and C. Laubschat, Phys. Rev. B **57**, 14930 (1998).

[15] N. Witkowski, F. Bertran, F. Dulot, D. Malterre, G. Panaccione, and A. Taleb, Eur. Phys. J. B **14**, 177 (2000).

[16] H. Tollefsen, L. J. Berstad, and S. Raaen, J. Vac. Sci. Technol. A **25**, 1433 (2007).

[17] C. J. Baddeley, A. W. Stephenson, C. Hardacre, M. Tikhov, and R. M. Lambert, Phys. Rev. B **56**, 12589 (1997).

[18] J. M. Essen, C. Becker, and K. Wandelt, J. Surf. Sci. Technol. **7**, 421 (2009).

[19] J. Libra and V. Matolín, Surf. Sci **600**, 2317 (2006).

[20] E. Beaurepaire, J. P. Kappler, S. Lewonczuk, J. Ringeissen, M. A. Khan, J. C. Parlebas, Y. Iwamoto, and A. Kotani, J. Phys.: Condens. Matter **5**, 5841 (1993).

[21] J. G. Sereni, O. Trovarelli, A. Herr, J. Ph. Schillé, E. Beaurepaire, and J. P. Kappler, J. Phys.: Condens. Matter **5**, 2927 (1993).

[22] Y. Iwamoto, M. Nakazawa, A. Kotani, and J. C. Parlebas, J. Phys.: Condens. Matter **7**, 1149 (1995).

[23] K. Kanai, Y. Tezuka, M. Fujisawa, Y. Harada, S. Shin, G. Schmerber, J. P. Kappler, J. C. Parlebas, and A. Kotani, Phys. Rev. B **55**, 2623 (1997).

[24] H. Hayashi, K. Shimada, J. Jiang, H. Iwasawa, Y. Aiura, T. Oguchi, H. Namatame, and M. Taniguchi, Phys. Rev. B **87**, 035140 (2013).

[25] K. D. Childs, B. A. Carlson, L. A. LaVanier, J. F. Moulder, D. F. Paul, W. F. Stickle, and D. G. Watson, *Handbook of Auger Electron Spectroscopy* (Physical Electronics Inc., Eden Prairie, MN, 1995).

[26] E. Malinowski, *Factor Analysis in Chemistry* (John Wiley & Sons, New York, 2002).

[27] S. Danzenbächer, Yu. Kucherenko, M. Heber, D. V. Vyalikh, S. L. Molodtsov, V. D. P. Servedio, and C. Laubschat, Phys. Rev. B **72**, 033104 (2005).

[28] S. Hüfner, *Photoelectron Spectroscopy* (Springer-Verlag, Berlin, 1995).

[29] F. Patthey, W. D. Schneider, Y. Baer, and B. Delley, Phys. Rev. B **34**, 2967 (1986).

[30] J. C. Fuggle, F. U. Hillebrecht, Z. Zolnierek, R. Lässer, Ch. Freiburg, O. Gunnarsson, and K. Schönhammer, Phys. Rev. B **27**, 7330 (1983).

[31] F. Patthey, J. M. Imer, W.-D. Schneider, H. Beck, Y. Baer, and B. Delley, Phys. Rev. B **42**, 8864 (1990).

[32] H. Schwab, M. Mulazzi, J. Jiang, H. Hayashi, T. Habuchi, D. Hirayama, H. Iwasawa, K. Shimada, and F. Reinert, Phys. Rev. B **85**, 125130 (2012).

[33] D. Malterre, M. Grioni, and Y. Baer, Adv. Phys. **45**, 299 (1996).

[34] S.-H. Yang, H. Kumigashira, T. Yokoya, A. Chainani, T. Takahashi, H. Takeya, and K. Kadowaki, Phys. Rev. B **53**, R11946(R) (1996).

[35] H.-D. Kim, H. Kumigashira, S.-H. Yang, T. Takahashi, H. Aoki, T. Suzuki, G. Chiaia, O. Tjernberg, H. Nylén, I. Lindau, and A. Ochiai, Phys. Rev. B **59**, 12294 (1999).

[36] S. Gardonio, T. O. Wehling, L. Petaccia, S. Lizzit, P. Vilmercati, A. Goldoni, M. Karolak, A. I. Lichtenstein, and C. Carbone, Phys. Rev. Lett. **107**, 026801 (2011).

[37] B. Horvatić, D. Šokčević, and V. Zlatić, Phys. Rev. B **36**, 675 (1987).

[38] M. T. Glossop and D. E. Logan, J. Phys.: Condens. Matter **14**, 6737 (2002).

[39] G. Czycholl, Phys. Rev. B **31**, 2867 (1985).